The outer valance orbital electron densities of cyclopentane by binary (*e,2e*) spectroscopy

J. K. Deng,[a] G. Q. Li, F. Wang, G. L. Su, C. G. Ning, T. Zhang, X. G. Ren, and Y. Wang
Department of Physics, Tsinghua University, Beijing 100084, People's Republic of China and Key Laboratory for Quantum Information and Measurements, MOE, People's Republic of China

Y. Zheng
Department of Chemistry, The University of British Columbia, Vancouver, British Columbia, V6T 1Z1, Canada

The binding energy spectra and electron distributions in momentum space of the valence orbitals of cyclopentane (C_5H_{10}) are studied by Electron Momentum Spectroscopy (EMS) in a noncoplanar symmetric geometry. The impact energy was 1200 eV plus binding energy and energy resolution of the EMS spectrometer was 1.2 eV. The experimental momentum profiles of the outer valence orbitals are compared with the theoretical momentum distributions calculated using Hartree–Fock and density functional theory (DFT) methods. The shapes of the experimental momentum distributions are generally quite well described by both the Hartree–Fock and DFT calculations when the large and diffuse basis sets are used. © *2004 American Institute of Physics.*
[DOI: 10.1063/1.1737296]

I. INTRODUCTION

Electron momentum spectroscopy (EMS) with symmetric noncoplanar geometry provides unique and detailed information on the electronic structures of atoms and molecules.[1–6] The technique can access the complete valence shell binding energy range, though with lower resolution than that in most photoelectron spectroscopy (PES) studies, and the orbital density imaging information provided by EMS momentum profiles is unique. In particular, the momentum distribution information, obtained by the EMS technique, provides stringent tests for quantum chemical calculations at the Hartree–Fock level and also of correlated treatments such as Density Functional Theory (DFT). The details of EMS experimental techniques and the associated theoretical analysis for atoms, molecules and condensed matter have been reviewed in detail elsewhere.[1,7–10]

Now a large body of EMS measurements is available for a wide variety of targets ranging from atoms to molecules.[10–15] These results have convincingly shown that the interplay of EMS measurements and high level quantum mechanical calculations provides very detailed information on the binding energy, electronic structure, reactivity and electron density distributions of electrons in atoms and molecules. In addition, it should be noted that the EMS technique is particularly sensitive to the low momentum part and thus the chemically important regions (i.e., outer spatial regions) of the outer valence (frontier) orbital electron density.

Up to now, the studies of the electronic structure of saturated hydrocarbon molecules have received much interest. This is because not only these molecules are prototypes of larger hydrocarbons, but also they are important species for fuels where reforming of straight chain hydrocarbons into branched chain species is of importance. As part of a series study of saturated hydrocarbon molecules using the high energy resolution EMS spectrometer at Tsinghua University,[13–16] we now report the measurements of orbital momentum profiles for the outer valence shell of cyclopentane (C_5H_{10}). The experiment was performed at impact energy of 1200 eV plus the binding energy using symmetric non-coplanar kinematics and the energy resolution was 1.2 eV. The measured results of the binding energy spectra are from 6 eV to 24 eV. The momentum profiles for the individual valence orbitals are obtained. A sufficiently high impact energy (>1200 eV) and momentum transfer were used to ensure the validity of the plane wave impulse approximation (PWIA). The relatively large number of electrons in cyclopentane renders accurate quantum chemical calculations quite difficult, thus the availability of good EMS experimental data is an important aid for developing satisfactory theoretical descriptions of both binding energies and the valence orbital electron densities in hydrocarbons.

Theoretical momentum distributions for valence orbitals are calculated using the target Hartree–Fock approximation (THFA) and also with the target Kohn–Sham approximation (TKSA).[1–6] In Hartree–Fock calculation, basis sets STO-3G, 6-311G, and 6-311++G** are used. In the DFT calculations, hybrid functionals B3LYP and BLYP are used. The measured momentum profiles are compared with the HF and DFT calculations. In general, experiment and theory are in very good agreement, but a difference between theory and experiment in the outer valance orbital is observed.

II. THEORETICAL BACKGROUND

In a binary (*e,2e*) experiment, the scattered and the ionized electrons are detected at the same kinetic energies and the same polar angles in symmetric noncoplanar scattering geometry. Under conditions of high impact energy and high

---
[a]Electronic mail: djk-dmp@mail.tsinghua.edu.cn

momentum transfer, the target electron essentially undergoes a clean ''knock-out'' collision and the plane wave impulse approximation (PWIA) provides a very good description of the collision. In the PWIA, the momentum p of the electron prior to knock-out is related to the azimuthal angle by[1]

$$p = [(2p_1 \cos \theta_1 - p_0)^2 + (2p_1 \sin \theta_1 \sin(\phi/2))^2]^{1/2}, \quad (1)$$

where $p_1 = p_2 = \sqrt{2E_1}$ is the magnitude of the momentum of each outgoing electron and $p_0 = \sqrt{2E_0}$ is the momentum of the incident electron (both in atomic units). The EMS differential cross section in the PWIA for randomly oriented gas-phase molecules is given by[1]

$$\sigma_{EMS} \propto \int |\langle \mathbf{p}\Psi_f^{N-1}|\Psi_i^N\rangle|^2 d\Omega, \quad (2)$$

where $\mathbf{p}$ is the momentum of the target electron state prior to knockout, $|\Psi_f^{N-1}\rangle$ and $|\Psi_i^N\rangle$ are the total electronic wave functions for the final ion state and the target molecule ground (initial) state, respectively. The overlap of the ion and neutral wave functions in Eq. (2) is known as the Dyson orbital while the square of this quantity is $|\langle \mathbf{p}\Psi_f^{N-1}|\Psi_i^N\rangle|^2$ and is referred to as an ion-neutral overlap distribution (OVD) or Dyson orbital momentum density distribution. Thus, the EMS cross section is essentially proportional to the spherical average ($\int d\Omega$) of the square of the Dyson orbital in momentum space.

Therefore, Eq. (2) is greatly simplified by using the target Hartree–Fock approximation (THFA). Within the THFA, the many-body wave functions $|\Psi_f^{N-1}\rangle$ and $|\Psi_f^N\rangle$ are approximated as independent particle determinants of ground state target Hartree–Fock orbitals. The ion state is then in most cases dominated by a single hole in only one orbital and Eq. (2) can be simplified to

$$\sigma_{EMS} \propto \int |\psi_j(\mathbf{p})|^2 d\Omega, \quad (3)$$

where $\psi_j(\mathbf{p})$ is the one-electron momentum space canonical Hartree–Fock orbital wave function for the jth electron, corresponding to the orbital from which the electron was ionized. The integral in Eq. (3) is known as the spherically averaged one-electron momentum distribution (MD). Equation (2) has also been interpreted in the context of Kohn–Sham density functional theory.[17] The target Kohn–Sham approximation (TKSA) gives a result similar to Eq. (3) in which the canonical Hartree–Fock orbital is replaced by a momentum space Kohn–Sham orbital $\psi_j^{KS}(\mathbf{p})$:

$$\sigma_{EMS} \propto \int |\psi_j^{KS}(\mathbf{p})|^2 d\Omega. \quad (4)$$

It should be noted that an accounting of electron correlation effects in the target ground state is included in the TKSA via the exchange correlation potential. A more detailed description of the TKSA-DFT method may be found elsewhere.[17] The TKSA approach has been compared with near Hartree–Fock limit and MRSD-CI overlap calculations and EMS measurements for the experimental momentum profiles of a large number of molecules (see, for example, Refs. 10–15).

In the present work, spherically averaged theoretical momentum profiles have been calculated for the valence orbitals of cyclopentane using the PWIA. Details of the calculation methods are described below and the total number of contracted Gaussian-type orbital functions (CGTO) is also given for each calculation. The Hartree–Fock and DFT calculations were carried out using the GAUSSIAN 98 program. The Hartree–Fock calculations of the momentum profiles were performed by using Eq. (3) with the basis sets of STO-3G 6-311G, and 6-311++G**. The B3LYP and BLYP functionals[18,19] are used for the two DFT calculations, respectively. Two basis sets of 6-311G and 6-311++G** are used for the DFT calculations.

A. STO-3G

A calculation employing a minimal basis set (effectively single zeta). Each function is a contraction of three Gaussian functions and thus it consists of $C(6s,3p)/[2s,1p]$ and $H(3s)/[1s]$ contractions. Therefore, a total of 35 CGTO is employed for cyclopentane. This basis set was designed by Pople and co-workers.[20]

B. 6-311G

The 6-311G basis of Pople and the co-workers[21] is comprised of an inner valence shell of six s-type Gaussians and an outer valence shell that has been split into three parts represented by three, one and one primitives, respectively. Carbon atoms have a $(11s,5p)/[4s,3p]$ contraction and hydrogen atoms have a $(5s)/[3s]$ contraction. A total of 95 CGTO is used for cyclopentane.

C. 6-311++G**

The 6-311++G** is an augmented version by Pople *et al.* Very diffused s- and p-functions, and spherical d-type polarization functions are added for carbon atoms, the full set of $6d$ Cartesian d functions have been used in the 6-311G** basis set. And a diffused sp shell and p-type polarization functions are added for hydrogen atoms.[22–24] Thus a $(12s,6p,1d)$ contracts to $[5s,4p,1d]$ for C, and a $(6s,1p)$ to $[4s,1p]$ for H. The number of CGTO is 185 for cyclopentane.

III. EXPERIMENTAL METHOD

The details and operation of the symmetric noncoplanar, energy dispersive, multichannel EMS spectrometer used in this work have been described in detail[25] and thus only a brief outline will be given here. The gas-phase target molecules ($\sim 10^{-5}$ Torr) are ionized by impact with a high energy electron beam ($E_0 = 1200$ eV plus binding energy). Two outgoing electrons (scattered and ionized) are electron optically retarded, selected energetically by electrostatic analyzers and detected in coincidence by microchannel plate position sensitive detectors mounted on two independent horizontal concentric turntables. In the symmetric noncoplanar scattering geometry, the two outgoing electrons are selected to have equal polar angles ($\theta_1 = \theta_2 = 45°$) relative to the forward scattered electron beam. One analyzer turntable is kept in a fixed position while the other is rotated by a computer controlled stepping motor. Each electron energy

J. Chem. Phys., Vol. 120, No. 21, 1 June 2004

Electron densities of cyclopentane   10011

analyzer accepts a range of kinetic energies from 596 to 604 eV simultaneously, but only those coincident electron pairs with summed energies in the range of 1200 ± 3.5 eV are recorded.

In present EMS measurements the individual orbitals are selected by the choice of the binding (or ionization) energy. In order to obtain the experimental momentum profiles corresponding to the main peaks with the multichannel energy dispersive spectrometer, wide range binding energy spectra (BES) are collected at a series of azimuthal (out of plane) angles ϕ over the range of 0° to $\pm 30°$ in a series of sequential repetitive scans.

Momentum distributions as a function of angle ϕ are obtained by deconvolution of these binding energy spectra using Gaussian functions located at each ionization energy in the BES. The widths and relative position of the Gaussian functions can be determined from a consideration of published high resolution PES vibronic manifolds and the EMS instrumental energy resolution function (1.2 eV FWHM). For each ionization process, the area of the fitted peak (or the integral of the spectral region, where appropriate) is plotted as a function of momentum calculated from ϕ using Eq. (1). A given set of areas as a function of momentum for a specific binding energy is referred to as an experimental momentum profile (XMP). To compare the XMPs with the relative cross sections calculated as a function of momentum using expressions (2) and (3) above, the effects of the finite spectrometer acceptance angles in both θ and ϕ ($\Delta\theta = \pm 0.6°$ and $\Delta\phi = \pm 1.2°$) were included in the calculations. This is achieved in the present work by using the Gaussian-weighted planar grid method of Duffy et al.[25] Due to finite angular resolution is generally small, the momentum profiles incorporated angular resolution only have small effect in the low momentum region. After momentum resolution folding, the calculation [Eqs. (2), (3) or (4)] is referred to as a theoretical momentum profile (TMP). The molecular geometry used in all calculations for cyclopentane was from Adams.[26]

All multichannel measurements in the present work were obtained using the "binning" mode.[27] The cyclopentane sample was reagent grade (>99.0% purity) and was used without further purification other than freeze–thaw cycles to remove dissolved air. No impurities were observed in any of the binding energy spectra.

IV. RESULTS AND DISCUSSION

Cyclopentane belongs to the D_{5h} point group and the Hartree–Fock (independent particle) ground state valence electron configuration can be written as

$$(1a_1')^2(1e_1')^4(1e_2')^4(2a_1')^2(2e_1')^4(2e_2')^4(3a_1')^2$$

$$(1a_2'')^2(1e_1'')^4(3e_2')^4(3e_1')^4(1e_2'')^4.$$

In the ground state, the forty electrons are arranged in twenty doubly occupied orbitals in the independent particle description. The valence electrons in cyclopentane are distributed in fifteen molecular orbitals and six of the orbitals are degenerate.

To obtain the experimental momentum profiles, twelve binding energy spectra over the energy range of 6–24 eV
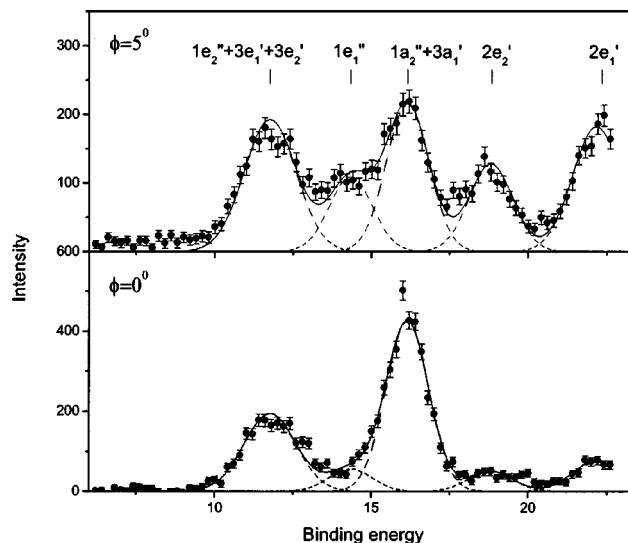
FIG. 1. EMS binding energy spectra of cyclopentane from 6 to 24 eV at $\phi = 0°$ (bottom) and 5° (top), obtained at an impact energy of 1200 eV plus binding energy. The dashed lines represent Gaussian fits to the peaks and the solid curve is the summed fit.

were collected at the out-of-plane azimuthal angles $\phi = 0°$, 1°, 2°, 3°, 4°, 5°, 7°, 9°, 11°, 13°, 16°, and 21° in a series of sequential repetitive scans. Figure 1 shows the valence shell binding energy spectra of cyclopentane in the range of 6–24 eV at the ϕ angles 0° and 5° at the impact energy of 1200 eV plus the binding energy. The spectra in Fig. 1 were fitted with a set of Gaussian peaks whose widths are combinations of the EMS instrumental energy resolution and the corresponding Franck–Condon widths derived from high resolution PES data.[28] The fitted Gaussians for individual peaks are indicated by dashed lines while their sum, i.e., the overall fitted spectra, are represented by the solid lines. The relative energy values are given by the relative ionization energies determined by high resolution PES. The energy scale in Fig. 1 was calibrated with respect to the $(1e_1'')^{-1}$ vertical ionization potential as measured by high resolution photoelectron spectroscopy.[28] The relative energy spacings of the Gaussian peaks were estimated from the vertical ionization potentials, with small adjustments to compensate for the asymmetries in the shapes of the Franck–Condon envelopes. The measured ionization potentials of this work and early published data[28–30] and the Hartree–Fock values are compared in Table I. Experimental data and theoretical values have been placed on a common intensity scale by normalizing the experimental to the DFT-B3LYP/6-311++G** theoretical momentum profiles for the $1e_1''$ orbital and the relative normalization is preserved for other orbitals.

The three outer-valence orbitals, $1e_2''$, $3e_1'$, and $3e_2'$, are not well separated experimentally due to their small energy separations. The band located at 14.35 eV corresponds to the ionization of the $1e_1''$ orbital. The next two valence orbitals $1a_2''$, $3a_1'$ are not well separated experimentally due to their small energy separations. The ionization peaks for the two inner valence orbitals, $2e_2'$, and $2e_1'$, are at 18.85 and 22.35 eV, respectively.

Experimental and theoretical spherically averaged mo-

TABLE I. Ionization energies (eV) for cyclopentane.

Orbital	Experiment[a]				Theoretical orbital energies of HF/6-311++G** [c]
	EMS[c]	PES[d]	PES[e]	XPS[f]	
$1e_2''$		11.01			11.824
$3e_1'$	11.77[a]	11.82			12.961
$3e_2'$		12.0			12.964
$1e_1''$	14.35	14.21			15.151
$1a_2''$	16.16[b]	15.96			17.406
$3a_1'$		16.5			17.478
$2e_2'$	18.85		18.29	18.40	20.928
$2e_1'$	22.35		22.2	22.07	26.087
$2a_1'$				25.31	30.027

[a]The peak of $1e_2''$, $3e_1'$, and $3e_2'$ orbitals.
[b]The peak of $1a_2''$ and $3a_1'$ orbitals.
[c]This work.
[d]Reference 28.
[e]Reference 29.
[f]Reference 30.

FIG. 2. Measured and calculated spherically averaged momentum profiles for the sum of the $1e_2''$, $3e_1'$, and $3e_2'$ orbitals of cyclopentane. The solid circles represent the experimental energy dispersive multichannel measurements. All calculations have been spherically averaged and folded with the experimental momentum resolution.

mentum profiles have been obtained for the valence orbitals of cyclopentane. Experimental momentum profiles (XMPs) are extracted by deconvolution of the sequentially obtained, angular-correlated, multichannel (binning mode) binding energy spectra. The Gaussian fitting procedure, described above for the binding energy spectra, is used to determine the relative intensities of the various orbital ionizations at each azimuthal angle ϕ. The experimental momentum profile for a particular orbital is obtained by plotting the area under the corresponding fitted peak for each electronic state of the ion as a function of p. Various theoretical momentum profiles (TMPs) of the valence orbitals are obtained with the methods described in Sec. II and the experimental instrumental angular resolutions have been incorporated in the calculations using the GW-PG method.[31]

The theoretical and experimental momentum profiles of the valence orbitals of cyclopentane are presented in Figs. 2–4. In the following discussion the comparisons between the theoretical calculations and the experimental data are provided for the valence orbitals.

The first peak of cyclopentane at 11.77 eV in the binding energy spectrum in Fig. 1 is associated with the $1e_2''$, $3e_1'$, and $3e_2'$ electrons. These orbitals are not well separated experimentally due to their small energy separations. Therefore, summed momentum distributions of the $1e_2''$, $3e_1'$, and $3e_2'$ orbitals are discussed for comparison between experiment and theory. Figure 2 shows that the summed XMPs has a double-peak distribution peaked at ~0.25 and ~1.0 a.u., respectively. The experimental intensity of the first peak is greater than the second one in the momentum distribution. According to the HF and DFT-B3LYP calculations, the $1e_2''$ orbital has a "p-type" distribution, $3e_1'$ orbital has a " $p-p$-type" distribution and the $3e_2'$ orbital has a "p-type" distribution, as shown under the summed momentum distribution curves in Fig. 2. The summed theoretical momentum distribution of these three orbitals therefore has a double-peak distribution. But, the comparison of the summed XMPs with various calculations in Fig. 2 shows that there is a significant discrepancy between experiment and theory. The dis-

crepancy between experiment and theory is probably due to inaccuracies in the Gaussian fitting procedures since these orbitals are not well separated. Another possible reason for the discrepancy could be because of the molecular geometry used in all calculations for cyclopentane. The well-balanced pentagon structure for cyclopentane[26] is used in this work, but that five carbon molecules of cyclopentane were not located at the same plane was reported in other paper.[32]
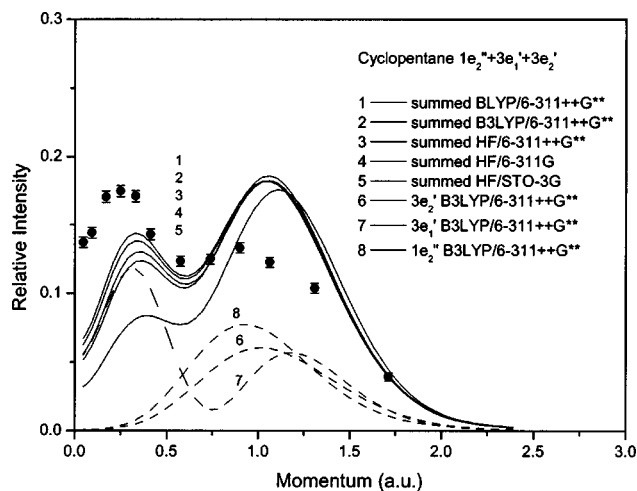
The experimental and the theoretical momentum profiles for the $1e_1''$ orbital of cyclopentane are shown in Fig. 3. The experimental and the theoretical momentum profiles show the expected p-type distribution (the experimental p_{max} ~0.7 a.u.). The four TMPs (curves 1–4) are very similar and fit to the XMPs very well in the momentum region above 0.3 a.u. However, there is a discrepancy between theoretical calculation and experimental data below the momentum of 0.3
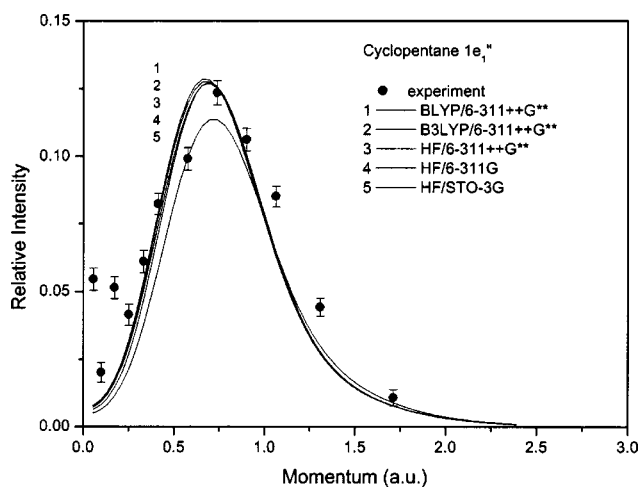
FIG. 3. Measured and calculated spherically averaged momentum profiles for the $1e_1''$ orbital of cyclopentane. The solid circles represent the experimental energy dispersive multichannel measurements. All calculations have been spherically averaged and folded with the experimental momentum resolution.

J. Chem. Phys., Vol. 120, No. 21, 1 June 2004

Electron densities of cyclopentane   10013
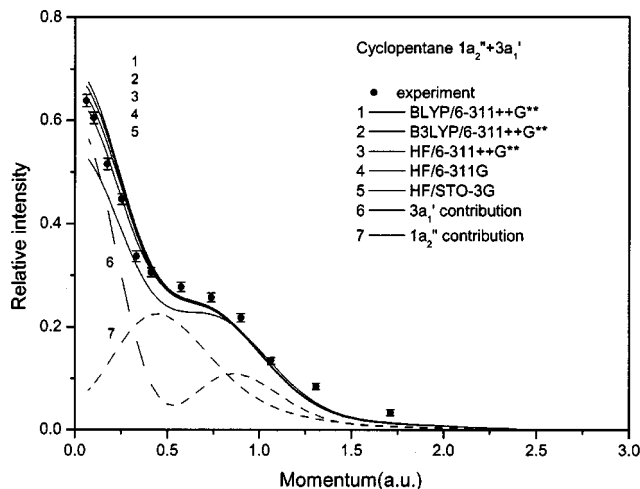
FIG. 4. Measured and calculated spherically averaged momentum profiles for the sum of the $1a_2''$ and $3a_1'$ orbitals of cyclopentane. The solid circles represent the experimental energy dispersive multichannel measurements. All calculations have been spherically averaged and folded with the experimental momentum resolution.

a.u. and all calculations underestimate the experimental intensity. The discrepancy between experiment and theory in the low momentum region is probably due to inaccuracies in the Gaussian fitting procedures since the nearby two ionization peaks are very close, and some intensity of the nearby peaks could leak into the $1e_1''$ peak in the low momentum range. Another possible source for the discrepancy in the low momentum range could be because of the distorted wave effects since the $1e_1''$ orbital of cyclopentane is a π^*-like molecular orbital. It has been found[15,16,33–35] that such orbitals usually produce a "turn-up" of the cross section in the low momentum range, and this behavior is similar to the low-p effect observed in atomic d-orbital XMPs. This situation is also probably the case for the $1e_1''$ orbital of cyclopentane. Such effects in atoms have been attributed to distorted wave effects that increase the calculated cross sections at low p as observed in the experimental measurements.[33] Similar behavior has been seen in the XMPs of transition-metal hexacarbonyl HOMOs that are known to be largely metal nd in character.[36] The corresponding transition-metal atoms show such behavior and this is found to decrease with increase in impact energy[36] in the distorted wave impulse approximation (DWIA) calculations. Unfortunately at present DWIA calculations are possible only for atoms but not for molecules due to the multicenter nature of the latter.

The third peak of cyclopentane at 16.16 eV in the binding energy spectrum in Fig. 1 contain contributions from the $1a_2''$, and $3a_1'$ orbitals. Summed experimental and theoretical momentum profiles for the $1a_2''$, and $3a_1'$ orbitals are shown in Fig. 4. The $1a_2''$ orbital has a "p-type" character (curve 7) while the $3a_1'$ orbital shows an "$s–p$-type" distribution (curve 6). The summed momentum profile is therefore a mixed "$s–p$-type" distribution. It can be seen from the comparison in Fig. 4 that the summed TMPs well reproduce the XMP except for the lower level calculation HF/STO-3G (curve 5) in the low momentum region.

V. SUMMARY

In summary, the detailed experimental and theoretical investigations of the outer valence orbital electron densities of cyclopentane by electron momentum spectroscopy are reported. The experimental momentum distributions are compared with the associated calculations. The binding energies are in excellent agreement with previously published PES data. The experimental momentum profiles are described by Hartree–Fock 6-311++G** calculations, and the density functional theory (DFT) calculations using B3LYP and BLYP functions provide the best description to the experiments.

[1] I. E. McCarthy and E. Weigold, Rep. Prog. Phys. **91**, 789 (1991), and references therein.
[2] C. E. Brion, Int. J. Quantum Chem. **29**, 1397 (1986).
[3] C. E. Brion, in *The Physics of Electronic and Atomic Collisions*, edited by T. Anderson *et al.* (American Institute of Physics, New York, 1993), p. 350.
[4] C. E. Brion, G. Cooper, Y. Zheng, I. V. Litvinyuk, and I. E. McCarthy, Chem. Phys. **270**, 13 (2001).
[5] K. T. Leung, in *Theoretical Models of Chemical Bonding*, edited by Z. B. Maksic (Springer-Verlag, Berlin, 1991), p. 339.
[6] A. O. Bawagan, C. E. Brion, E. R. Davison, and D. Fellar, Chem. Phys. **113**, 19 (1987).
[7] I. E. McCarthy, Aust. J. Phys. **51**, 593 (1998).
[8] M. A. Coplan, J. H. Moore, and J. P. Doering, Rev. Mod. Phys. **66**, 985 (1994).
[9] M. Vos and I. E. McCarthy, Rev. Mod. Phys. **67**, 713 (1995).
[10] Y. Zheng, J. J. Neville, and C. E. Brion, Science **270**, 786 (1995).
[11] I. V. Litvinyuk, Y. Zheng, and C. E. Brion, Chem. Phys. **261**, 289 (2000).
[12] I. V. Litvinyuk, J. B. Young, Y. Zheng, G. Cooper, and C. E. Brion, Chem. Phys. **263**, 195 (2001).
[13] J. K. Deng, G. Q. Li, J. D. Huang *et al.*, Chem. Phys. Lett. **313**, 134 (1999).
[14] J. K. Deng, G. Q. Li, Y. He *et al.*, J. Chem. Phys. **114**, 882 (2001).
[15] J. K. Deng, G. Q. Li, X. D. Wang, J. D. Huang, H. Deng, C. G. Ning, Y. Wang, and Y. Zheng, J. Chem. Phys. **117**, 4839 (2002).
[16] J. K. Deng, G. Q. Li, J. D. Huang *et al.*, Chin. Phys. Lett. **19**, 47 (2002).
[17] P. Duffy, D. P. Chong, M. E. Casida, and D. R. Salahub, Phys. Rev. A **50**, 4707 (1994), and references therein.
[18] J. P. Perdew and Y. Wang, Phys. Rev. B **33**, 8800 (1986).
[19] A. D. Becke, Phys. Rev. A **38**, 3098 (1988).
[20] W. J. Hehre, R. F. Stewart, and J. A. Pople, J. Chem. Phys. **51**, 2657 (1969).
[21] R. Krishnan, M. J. Frisch, and J. A. Pople, J. Chem. Phys. **72**, 4244 (1980).
[22] T. Clark, J. Chandrasekhar, G. W. Spitznagel, and P. V. R. Schleyer, J. Comput. Chem. **4**, 294 (1983).
[23] M. J. Frisch, J. A. Pople, and J. S. Binkley, J. Chem. Phys. **80**, 3265 (1984).
[24] T. H. Dunning, Jr., J. Chem. Phys. **90**, 1007 (1989).
[25] Y. Zheng, W. N. Pang, R. C. Shang, X. J. Chen, C. E. Brion, T. K. Ghanty, and E. R. Davidson, J. Chem. Phys. **111**, 9526 (1999).
[26] W. J. Adams, H. J. Geise, and L. S. Bartell, J. Am. Chem. Soc. **92**, 5013 (1970).
[27] Y. Zheng, J. J. Neville, C. E. Brion, Y. Wang, and E. R. Davidson, Chem. Phys. **188**, 109 (1994).
[28] K. Kimura, S. Katsumata, Y. Achiba, T. Yamazaki, and S. Iwata, *Handbook of HeI Photoelectron Spectra of Fndamental Organic Molecules* (Japan Scientific Society, Tokyo, 1981).

10014   J. Chem. Phys., Vol. 120, No. 21, 1 June 2004

Deng *et al.*

[29] A. W. Potts and D. Streets, J. Chem. Soc., Faraday Trans. 2 **70**, 875 (1974).

[30] M. Deleuze, J. Delhalle, B. T. Pickup, and S. Svensson, J. Am. Chem. Soc. **116**, 10715 (1994).

[31] P. Duffy, M. E. Casida, C. E. Brion, and D. P. Chong, Chem. Phys. **159**, 347 (1992).

[32] M. Deleuze, J. Delhalle, and B. T. Pickup, J. Phys. Chem. **98**, 2382 (1994).

[33] C. E. Brion, Y. Zheng, J. Rokle, J. J. Neville, I. E. McCarthy, and J. Wang, J. Phys. B **31**, L223 (1998).

[34] J. Rolke, Y. Zheng, C. E. Brion, Z. Shi, S. Wolfe, and E. R. Davidson, Chem. Phys. **244**, 1 (1999).

[35] M. J. Brunger, S. W. Braidwood, I. E. McCarthy, and E. Weigold, J. Phys. B **27**, L597 (1994).

[36] J. Rolke, Y. Zheng, C. E. Brion, S. J. Chakravorty, E. R. Davidson, and I. E. McCarthy, Chem. Phys. **215**, 191 (1997).